# Shear Induced Isotropic-to-Lamellar Transition in a Lattice-Gas Automaton Model of Microemulsions.

Andrew N. Emerton

*Department of Theoretical Physics, Oxford University,*

*1 Keble Road, Oxford OX1 3NP, U.K.*

Peter V. Coveney

*Schlumberger Cambridge Research,*

*High Cross, Madingley Road, Cambridge CB3 0EL, UK.*

Bruce M. Boghosian

*Center for Computational Science, Boston University,*

*3 Cummington Street, Boston, Massachusetts 02215, U.S.A.*

February 18, 1997

**Abstract**

We report on the simulation of an isotropic-to-lamellar transition under linear shear flow in a ternary system of oil, water and surfactant. This experimentally observed and theoretically predicted behaviour has not been simulated before. We are able to model the phenomenon by using our recently introduced lattice-gas automaton model of amphiphilic systems, which is well suited for simulating complex multi-phase flows of this nature.

PACS numbers: 82.70.-y;05.70.Lm

## 1 Introduction

Soft materials such as polymer solutions, liquid crystals, surfactants, and microemulsions are frequently processed or utilized through the application of large deformations. Various attempts have been made to investigate and characterize the behaviour of such complex systems under conditions such as shear flow where the industrial applications are clear [1]. In this letter we model the effect of linear shear flow on a fully hydrodynamic, isotropic, bicontinuous microemulsion phase using our recently introduced lattice-gas automaton model for simulating self-assembling amphiphilic systems

[2]. Experimental results [3] and theoretical predictions [4] support evidence for the presence of a transition from an isotropic to a lamellar phase in such systems; however, we are unaware of any model that is capable of *simulating* complex multi-phase flow of this sort. This is because of the considerable difficulty involved in simulating ternary microemulsion systems under hydrodynamic flow, as well as in the implementation of the boundary conditions required for shear; traditional fluid-dynamical modelling techniques, such as computational fluid dynamics or molecular dynamics cannot viably deal with the complexity involved.

Lattice-gas models automaton have evolved from simulating simple one-component Navier-Stokes fluids [5], to two and multi-component immiscible lattice-gas models [6], which we have recently extended to a system including amphiphilic particles [2]. Lattice-gas automaton models can reproduce fluid dynamics on mesoscopic scales, permitting the investigation of non-equilibrium (kinetic) behaviour over a broad range of length and time scales [7]. The relative simplicity of the collision rules, the implicit complex interface formation, the natural underlying kinetic fluctuations and the ease of implementation of complex boundary conditions suggest that lattice-gas automata are an appropriate choice for the present application to the study of microemulsion phases under linear shear.

Linear shear flow has previously been applied to binary fluid systems in both two [8] and three-dimensional [9] lattice-gas models. We make use of the method introduced in the second of these papers for obtaining linear shear flow on the lattice, although some modification is required for our ternary microemulsion system.

As well as simulating the isotropic-to-lamellar transition for the first time, this work was undertaken in order to further investigate the validity of our amphiphilic model for complex fluid simulation. This is the first application of the model to the simulation of known physical effects associated with bulk fluid flow. In Section 2 we briefly describe our model and the numerical techniques we have used to investigate the system under shear; our simulations are presented in Section 3 with concluding remarks in Section 4.

## 2 Model and Analysis

We perform simulations using our basic lattice-gas model of amphiphilic systems as previously published [2]. The model is a microscopic dynamical system which gives the correct mesoscopic and macroscopic behaviour of mixtures of oil, water and surfactant. The model is based on the two-fluid immiscible lattice-gas of Rothman and Keller [10] which we have reformulated using a microscopic particulate description to permit the inclusion of amphiphile. The model exhibits the commonly formed equilibrium microemulsion phases, including droplets, bicontinua and lamellae [2]. Moreover, the model conserves momentum as well as the masses of the various species, and correctly simulates the fluid dynamical and scaling behaviour during self-assembly of these phases [11].

In order to incorporate the most general form of interaction energy (Hamiltonian) within our model system, we introduce a set of coupling constants $\lambda, \mu, \epsilon, \zeta$, in terms of which the total interaction energy can be written as [2]

$$\Delta H_{\mathrm{int}} = \lambda \Delta H_{\mathrm{cc}} + \mu \Delta H_{\mathrm{cd}} + \epsilon \Delta H_{\mathrm{dc}} + \zeta \Delta H_{\mathrm{dd}}. \tag{1}$$

The four terms on the right hand side correspond, respectively, to the relative immiscibility of oil and water, the tendency of surrounding surfactant to bend around oil or water droplets, the propensity of surfactant dipoles to align across oil-water interfaces and the contribution from pairwise interactions between surfactant molecules. For consistency we choose these coefficients to be of the same value for all simulations in this letter and to be those that allow a bicontinuous microemulsion phase to form in one part of the ternary phase diagram [2]: as such these are,

$$\lambda = 1.0, \mu = 0.05, \epsilon = 8.0, \zeta = 0.5. \tag{2}$$

In order to investigate the effect of linear shear flow on a bicontinuous microemulsion phase we apply a technique devised by Olson and Rothman [9] for shearing two-component binary lattice-gas fluids, which we have adapted to meet the requirements of our amphiphilic lattice-gas model. The technique provides a linearly varying, tunable velocity in a direction orthogonal to that of the flow. The velocities used are small enough so that the lattice-gas accurately represents the hydrodynamic flow [9].

We analyse the simulation results in three ways. The first is direct visualisation of the growth of domains both with and without the imposition of a shear velocity; the second, performed in order to observe any anisotropic domain growth in the case of shear, is a quantitative analysis of non-circularly averaged structure functions of the oil-water colour density difference,

$$S(\mathbf{k}, t) = \left\langle \frac{1}{N} \left| \sum_{\mathbf{x}} (q(\mathbf{x}) - q^{av}) e^{i\mathbf{k}\cdot\mathbf{x}} \right|^2 \right\rangle, \tag{3}$$

where $\mathbf{k} = (2\pi/L)\,(m\mathbf{i} + n\mathbf{j})$, $m, n = 1, 2, ..., L$, $q(\mathbf{x})$ is the total colour charge at a site, $q^{av}$ is the average value of the colour charge, $L$ is the length of the system and $N = L^2$ is the number of lattice sites in the system. Thirdly, we evaluate the values of the average $x$ and $y$ components of all the surfactant vectors in the system at any one time, namely:

$$X^2 = \sum_{\mathbf{x}} \left( \sum_i \sigma_{ix}^2(\mathbf{x}) \right), \tag{4}$$

and,

$$Y^2 = \sum_{\mathbf{x}} \left( \sum_i \sigma_{iy}^2 \mathbf{x} \right), \tag{5}$$

where $\sigma_{ix}$ is the $x$ component of the surfactant dipole vector moving in direction $i$ at lattice site $\mathbf{x}$, and similarly $\sigma_{iy}$ is the $y$ component of that vector.

As well as undertaking simulations both with and without a shear velocity present for the whole timescale of the run, we also investigate the case where the imposed velocity becomes non-zero only after a predetermined number of time-steps of the simulation, this is in order to verify that the transition to the lamellar phase can indeed be accessed from a perturbation of the equilibrium isotropic bicontinuous phase (as Cates and Milner assumed [4]) and is not just a shear-induced pattern of phase-separated fluid domains [12].

# 3 Simulations

As already discussed, we undertake simulations both with and without shear flow present in order for a critical comparison to be made; in the former case the shear velocity is introduced at two different stages during the simulations, at time-step 0 and time-step 5000 respectively. For all simulations reported on here we use reduced densities of water, surfactant and oil of 0.215, 0.1075 and 0.215 respectively, although we note that these are just one set of many in the vicinity that give the behaviour we describe below. The velocities that give rise to the shear flow are imposed on the left and right ($y$ direction) sides of the simulation box and are $-0.1$ and $0.1$ lattice units per time step respectively. We use a $2D$ lattice of size $128 \times 128$ with periodic boundary conditions in both directions for all simulations. In each case the initial condition is a random mixing of all three particle types in the system.

## 3.1 Absence of Shear

The first set of simulations are for the system with a shear velocity of zero throughout the timescale of the simulation. We find evidence of the usual bicontinuous microemulsion phase consisting of percolating tubular-like domains; the phase is clearly isotropic in nature.

The visualisations of this at selected time-steps are shown in Fig. 1. We have also calculated the non-circularly averaged structure function of the oil-water density at various points during the run. This is essential for later comparison with the case when shear is included; see Fig's 2 & 3. It is clear from these figures that the structure growth has no preference for any lattice direction, and provides quantitative evidence for the isotropic nature of the phase. Additionally, and as we found in our previous work [2], the domain structures do not grow in size indefinitely; rather, what we see is the development of an equilibrium bicontinuous phase; however, we note that the underlying lattice dynamics are still present. The characteristic size of the oil-water domains has stopped growing by about time-step 5000. The other measurement we make is of the total values $X^2$ and $Y^2$, of the $x$ and $y$ components of all surfactant vectors in the system at every time-step; again these values are calculated for later comparison with the case when shear is imposed. The values of these expressions at selected timesteps are shown in Table 1. In this no shear case, as expected, there is little difference between the $X$ and $Y$ components during the time-scale of the simulation, this being further evidence for the presence of an isotropic system.

### 3.2 Application of Shear

In the first case the system has a steady shear velocity of $\pm 0.1$ lattice-units per time-step in the $y$ direction of the simulation box for the whole timescale of the run.

The direct visual result we obtain is shown in Fig. 4. We also replicate the calculation of the non-circularly averaged structure function of the oil-water density at various time-steps during the run, see Fig's 5, 6 & 7. Additionally, as before, the other measurement we make is of the total values $X^2$ and $Y^2$ of the $x$ and $y$ components of all surfactant vectors at every timestep. The values of these expressions at selected timesteps are shown in Table 2.

All these results show very different behaviour from the case of no shear. The visual evidence shows lamellar-like structures forming early on in the simulation, although it is not until the late-time regime that the structures have stabilised to form individual layers which align with the ($y$) direction of the imposed linear shear flow. The non-circularly averaged structure functions, once the lamellar-like structures appear, show clear imbalance in their preferred direction and magnitude, the peak(s) becoming large at low ($\rightarrow 0$) values of $k_y$ and finite $k_x$, indicating periodic structures that extend (indefinitely - periodic boundary conditions) in the real-space $y$ lattice direction. The presence of two major peaks at time-steps 18800 and 27000 indicates that the characteristic size of the domains increases slightly as the more stable lamellar layers form; these begin to dominate over the initially thinner, slightly skewed layers that the impact of the shear flow initially creates. These results are indicative of the presence of a periodic lamellar structure which is obviously anisotropic, and are further supported by the disparity in the total $X^2$ and $Y^2$ values of the surfactant vectors: on average we expect the vectors to align at right angles to the oil-water interfaces, with $X^2 >> Y^2$ if the oil-water layers are aligned parallel to the $y$ lattice direction; this is indeed the case.

We have confirmed that the lamellar state is not a shear-induced pattern of phase separated fluid domains, but is actually a perturbed equilibrium phase, by imposing shear only after time-step 5000 has been reached in a simulation. The domain structure formed by this point is a bicontinuous equilibrium phase [2] which then comes under the influence of the shear flow. Although we now have to wait longer for the transition to occur, the system still evolves from the isotropic, equilibrium phase to the anisotropic lamellar state as we would expect (see for example Fig. 8).

# 4 Conclusions

Using our lattice-gas automaton model for amphiphilic systems, we have been able to simulate the transition from an isotropic bicontinuous to a lamellar phase in a ternary microemulsion system under the influence of linear shear flow. This effect has not been simulated previously and confirms that our model is capable of describing complex multi-phase fluid phenomena that is out of reach of other computer simulation methods. To link our results more fully with both experimental data and theoretical analysis, a detailed investigation of the complete non-equilibrium phase diagram of our model is needed and as such is an area for future work.

# Acknowledgments

We are grateful to Mike Cates and John Olson for helpful discussions during the development of this work. In particular, we thank John Olson for assistance in implimentating his shear methods within our model. One of us (ANE) wishes to thank EPSRC and Schlumberger for funding his CASE award; another of us (BMB) was supported in part by Phillips Laboratories and by the United States Air Force Office of Scientific Research under grant number F49620-95-1-0285. PVC and BMB thank NATO for the award of a collaborative grant.

# References

[1] Hoffmann H., *Adv. Mater.* **6** (1994) 116-129.

[2] Boghosian B.M., Coveney P.V. and Emerton A.N., *Proc. Roy. Soc. Lond. A.* **452** (1996) 1221-1250.

[3] Koppi K.A., Tirrell M. and Bates F.S., *Phys. Rev. Lett.* **70** (1993) 1449-1452.

[4] Cates M.E. and Milner S.T., *Phys. Rev. Lett.* **62** (1989) 1856-1859.

[5] Frisch U., Hasslacher B. and Pomeau Y., *Phys. Rev. Lett.* **56** (1986) 1505-1508.

[6] Gunstensen A.K. and Rothman D.H., *Physica D.* **47** (1991) 47-52.

[7] Rothman D.H. and Zaleski S., *Rev. Mod. Phys.* **66** (1994) 1417-1475.

[8] Rothman D.H., *Phys. Rev. Lett.* **65** (1990) 3305-3308.

[9] Olson J.F. and Rothman D.H., *J. Stat. Phys.* **81** (1995) 199-222.

[10] Rothman D.H. and Keller J.M., *J. Stat. Phys.* **52** (1988) 1119-1127.

[11] Emerton A.N., Coveney P.V. and Boghosian B.M., *Phys. Rev. E.* submitted (1996).

[12] Cates M.E., private communication (1996).

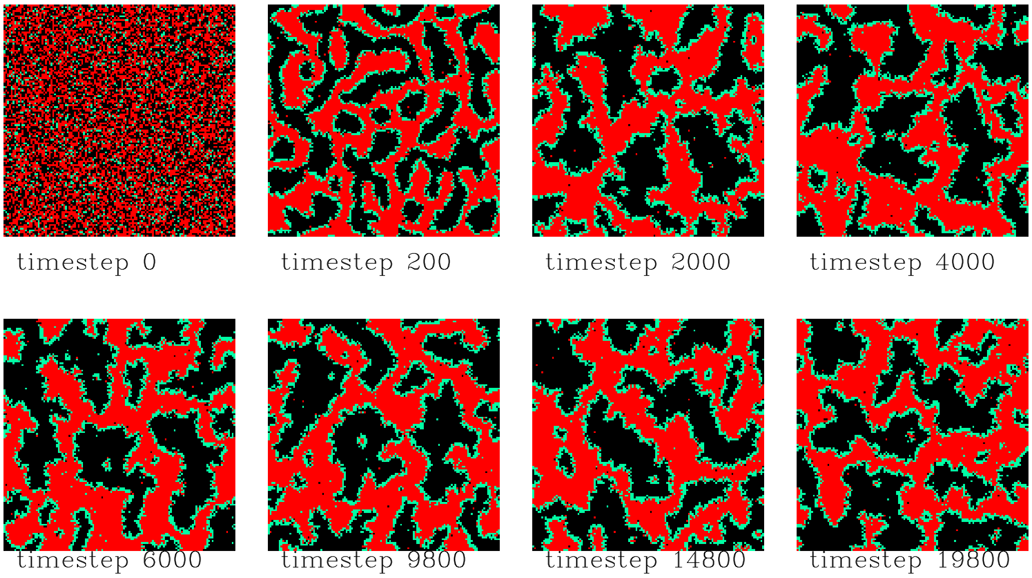


Figure 1: *Time evolution of bicontinuous microemulsion phase in absence of shear. The $x$ axis is along the horizontal and the $y$ axis along the vertical side of the simulation images shown here.*

| *Timestep* | $X^2$ | $Y^2$ |
|---|---|---|
| 200 | 3135.387 | 3255.134 |
| 1000 | 3108.330 | 3008.818 |
| 3000 | 3028.797 | 3098.200 |
| 6000 | 3177.268 | 3023.230 |
| 9800 | 3070.322 | 3078.127 |
| 18800 | 3037.269 | 3190.526 |

Table 1: *Total $X$ and $Y$ component values of surfactant dipole vectors at selected timesteps for the case of no shear.*

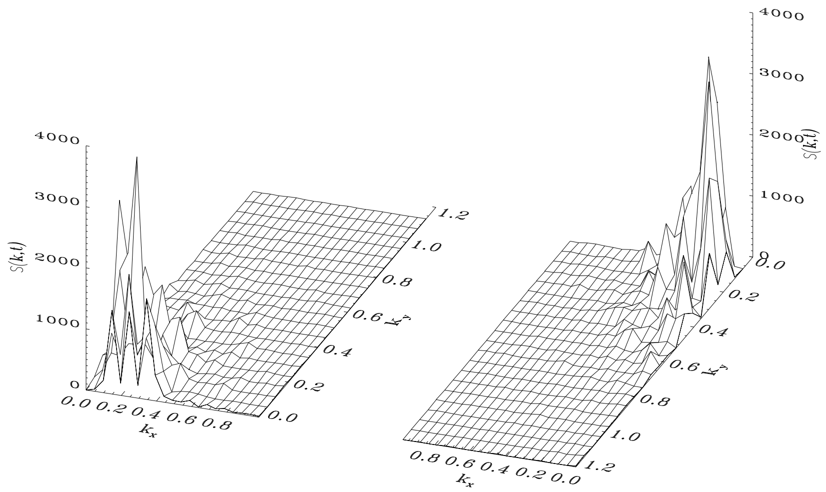


Figure 2: *Temporal evolution of $S(\mathbf{k}, t)$ for bicontinuous microemulsion case with no shear velocity. Timesteps depicted here are 1000 on the left-hand side and 3000 on the right. The axes on the right-hand figure are a mirror image of those on the left to aid visual clarity.*

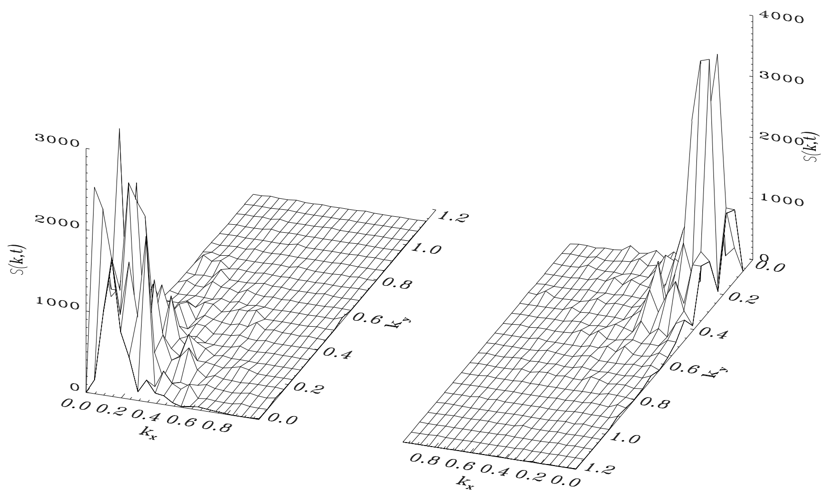


Figure 3: *Temporal evolution of $S(\mathbf{k}, t)$ for bicontinuous microemulsion case with no shear velocity. Timesteps depicted here are 9800 on the left-hand side and 16000 on the right. The axes on the right-hand figure are a mirror image of those on the left to aid visual clarity.*

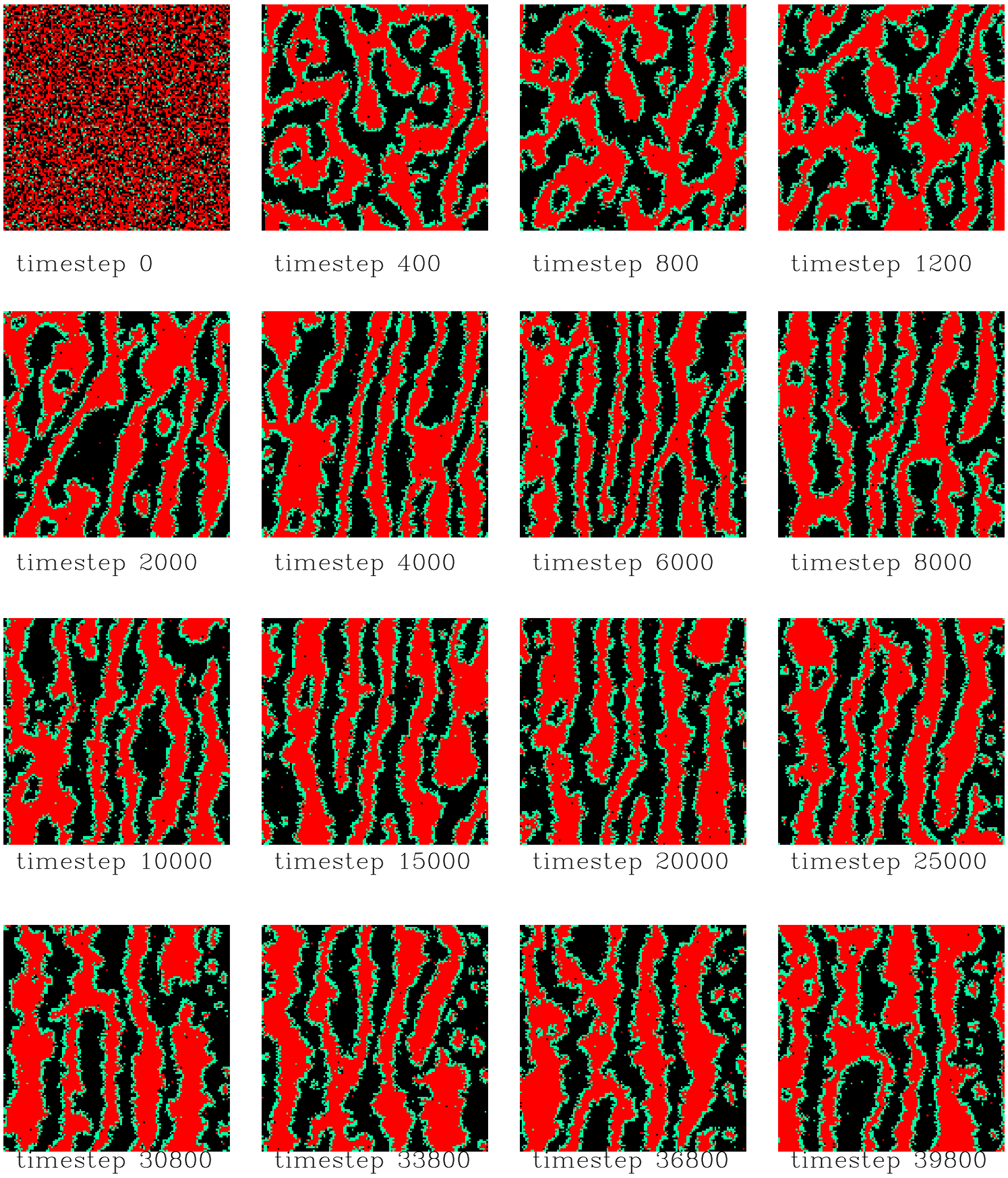


Figure 4: *Time evolution of microemulsion phase in the presence of shear. The $x$ axis is along the horizontal and the $y$ axis along the vertical side of the simulation images shown here. The imposed shear velocity is $\pm 0.1$ lattice units per time-step in the $y$ direction, $+0.1$ being on the right.*

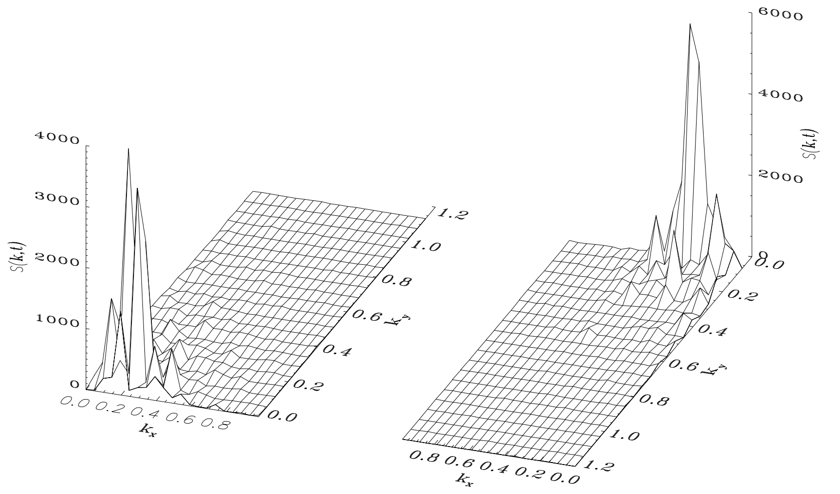


Figure 5: *Temporal evolution of $S(\mathbf{k},t)$ for bicontinuous microemulsion case with shear velocity. Timesteps depicted here are 1000 on the left-hand side and 3000 on the right. The axes on the right-hand figure are a mirror image of those on the left to aid visual clarity.*

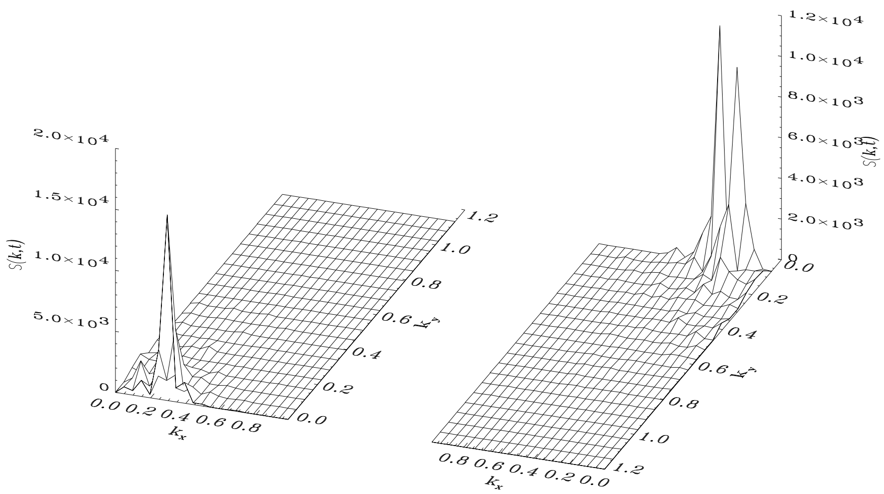


Figure 6: *Temporal evolution of $S(\mathbf{k},t)$ for bicontinuous microemulsion case with shear velocity. Timesteps depicted here are 9800 on the left-hand side and 18800 on the right. The axes on the right-hand figure are a mirror image of those on the left to aid visual clarity.*

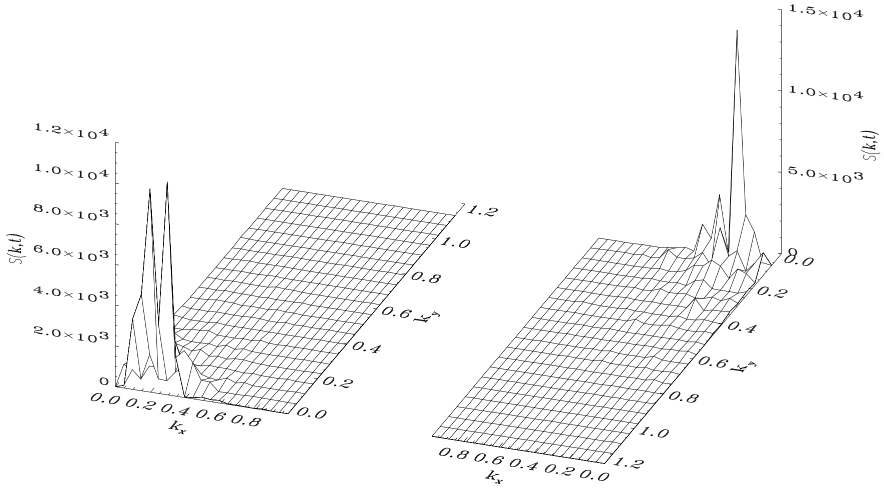


Figure 7: *Temporal evolution of* $S(\mathbf{k}, t)$ *for bicontinuous microemulsion case with shear velocity. Timesteps depicted here are* 27000 *on the left-hand side and* 39800 *on the right. The axes on the right-hand figure are a mirror image of those on the left to aid visual clarity.*

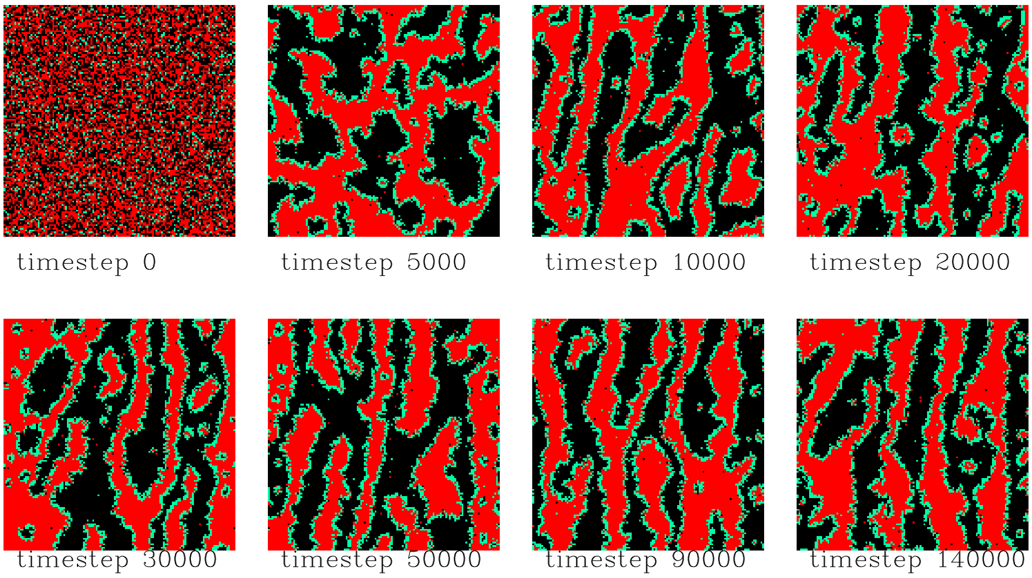


Figure 8: *Time evolution of microemulsion phase, shear imposed only after time-step* 5000*. The* $x$ *axis is along the horizontal and the* $y$ *axis along the vertical side of the simulation images shown here. The imposed shear velocity is* $\pm 0.1$ *lattice units per time-step in the* $y$ *direction,* $+0.1$ *being on the right.*

| *Timestep* | $X^2$ | $Y^2$ |
|---|---|---|
| 200 | 3305.145 | 2979.603 |
| 1000 | 3386.570 | 2804.306 |
| 3000 | 3858.108 | 2323.922 |
| 6000 | 4142.320 | 2132.849 |
| 9800 | 3744.983 | 2436.789 |
| 18800 | 3706.208 | 2416.251 |
| 28800 | 3744.401 | 2447.553 |
| 34800 | 3625.630 | 2537.532 |
| 39800 | 3629.221 | 2561.299 |

Table 2: *Total X and Y component values of surfactant dipole vectors at selected timesteps for the case of shear flow.*